Tong, T.W. and Sathe, S.B., 1991, "Heat Transfer Characteristics of Porous Radiant Burners". ASME Journal of Heat Transfer, 113, pp. 423-428.
Viskanta, R. and Gore, J.P., 2000, "Overview of Cellular Ceramics Based Porous Radiant Burners for Supporting Combustion", Clean Air. International Journal on Environmental Combustion Technologies, Vol.1, pp. 167-203.
Yanenko, N.N., 1971, "The Method of Fractional Time Steps: The Solution of Problems of Mathematical Physics in Several Variables". Ed. by M. Holt, Springer-Verlag, New York.

7. RESPONSIBILITY NOTICE

The authors are the only responsible for the printed material included in this paper.

burner operation facing a hot wall are higher than in the case of low temperature outlet boundary for all the operating conditions tested.

5. ACKNOWLEDGEMENTS

This work was partially supported by EC project ENK6-CT-2000-00317. T.C. Hayashi would like to thank the Fundação CAPES (Brasília, Brazil) for the PhD fellowship granted.

6. REFERENCES

Al-Hamamre, Z., Diezinger, S., Talukdar, P., Von Issendorff, F. and Trimis, D., 2006, "Combustion of Low Calorific Gases from Landfills and Waste Pyrolysis using Porous Medium Burner Technology", Process Safety and Environmental Protection, Vol.84, pp. 297-308.

Babkin, V.S., Korzhavin, A.A. and Bunev, A.A., 1991, "Propagation of Premixed Gaseous Explosion Flames in Porous Media", Combustion and Flame, Vol.87, pp.182-190.

Brehmer, T., Heger, F., Lucka, K., von Schloss, J., Abu-Sharekh, Y., Trimis, D., Heeb, A., Köb, G., Hayashi, T., Pereira, J.C.F., Founti, M., Kolaitis, D., Molinari, M., Ortona, A., Michel, J.-B. and Theurillat, P., 2003, "BIOFLAM Project: Application of Liquid Biofuels in New Heating Technologies for Domestic Appliances Based on Cool Flame Vaporization and Porous Medium Combustion", Proceedings of the 7th International Conference on Energy for a Clean Environment, Lisbon, Portugal.

Durst, F. and Trimis, D., 2002, "Combustion by Free Flames versus Combustion Reactors", Clean Air. International Journal on Energy for a Clean Environment, Vol.3, pp. 1-20.

Glarborg, P., Lilleheie, N.I., Byggstøyl, S., Magnussen, B.F., Kilpinen, P. and Hupa, M.,1992, "A Reduced Mechanism for Nitrogen Chemistry in Methane Combustion". Twenty-fourth Symposium (International) on Combustion, The Combustion Institute, Sidney, Australia, pp. 889-898.

Hayashi, T.C., 2005, "Multidimensional Modelling and Calculation of Combustion in Porous Media", PhD Thesis, Instituto Superir Técnico, Lisbon, Portugal, 206 p.

Hayashi, T.C., Malico, I. and Pereira, J.C.F., 2004, "Three-dimensional Modelling of a Two-layer Porous Burner for Household Applications", Computers and Structures, Vol.82, pp. 1543-1550.

Hayashi, T.C., Malico, I. and Pereira, J.C.F., 2007, "Influence of the Preheating Layer Characteristics in a Two-layer Porous Burner", accepted for publication on Clean Air. International Journal on Energy for a Clean Environment.

Hsu, P.-F., Evans, W.D. and Howell, J.R., 1993, "Experimental and Numerical Study of Premixed Combustion within Nonhomogeneous Porous Ceramics", Combustion Science and Technology, Vol.90, pp. 149-172.

Howell, J.R., Hall, M.J. and Ellzey, J.L., 1996,. "Combustion of Hydrocarbon Fuels within Porous Inert Media", Progress in Energy and Combustion Science, Vol.22, pp. 121-145.

Joynt, B., and Wu, S., 2000, "Nitrogen Oxides Emissions Standards for Domestic Gas Appliances – Background Study". 17 May, 2007 <www.deh.gov.au/atmosphere/air quality/publications/residential/noxconclusion.html>

Kaviany, M., 1995, "Principles of Heat Transfer in Porous Media", Springer-Verlag, New York, USA, 626 p.

Kee, R.J., Rupley, F.M., and Miller, J.A., 1995a, "CHEMKIN-II: a Fortran Chemical Kinetics Package for the Analysis of Gas-phase Chemical Kinetics". Sandia National Laboratories report SAND89-8009B.UC-706, Albuquerque, USA.

Kee, R.J., Dixon-Lewis, G., Warnatz, J., Coltrin, M.E., and Miller, J.A., 1995b, "A Fortran Computer Package for the Evaluation of Gas-phase Multicomponent Transport Properties". Sandia National Laboratories report SAND86-8246.UC-401, Albuquerque, USA.

Kotani, Y., Behbahani, H.F. and Takeno, T., 1984, "An Excess Enthalpy Flame Combustor for Extended Flow Ranges", Proceedings of the 20th Symposium (International) on Combustion, The Combustion Institute, pp. 1503-1509.

Lammers, F.A. and de Goey, L.P.H., 2003, "A Numerical Study of Flash Back of Laminar Premixed Flames in Ceramic-foam Surface Burners", Combustion and Flame, Vol.133, pp. 47-61.

Macdonald, I.F., El-Sayed, M.S., Mow, K. and Dullien, F.A.L., 1979, "Flow Through Porous Media – The Ergun Equation Revisited". Industrial Engineering Chemistry Fundamentals, 18, pp. 199-208.

Mital, R., Gore, J.P. and Viskanta, R., 1996, "Measurements of Radiative Properties of Cellular Ceramics at High Temperature". AIAA Journal of Thermophysics and Heat Transfer, 10, pp. 33-38.

Modest, M.F., 1993, "Radiative Heat Transfer". McGraw-Hill, Singapore, 832p.

Möβbauer, S., Pickenäcker, O., Pickenäcker, K. and Trimis, D., 1999, "Application of the Porous burner Technology in Energy- and Heat- Engineering", Proceedings of the 5th International Conference on Energy for a Clean Environment, Vol.1, Lisbon, Portugal, pp.519-523.

Őzişic, M.N., 1985, "Heat Transfer – A Basic Approach". McGraw-Hill Book Co., Singapore.

Patankar, S.V., 1980, "Numerical Heat Transfer and Fluid Flow". Hemisphere Publishing Corporation, New York, 197p.

accompanied by an increase in the CO formed. This is due to the favouring of the reaction of dissociation of CO_2 at higher temperatures. Excess air ratio influences the production of CO in the opposite direction, i.e., emission of this pollutant decreases rapidly when the dilution of the reactants mixture is increased at a constant power. This is due to the increased availability of oxygen, which favours the completion of the combustion process with reduction of intermediate species in the outflow from the burner.

The results for the burner radiating to the environment suggest that there is an optimum excess air ratio, around 1.2, for which the CO emission from the burner is minimized. Apart from this optimum air-to-fuel ratio, emissions increase. For richer mixtures, this is due to reduction in the availability of the oxidant agent. For mixtures with higher excess air ratio, an analysis of the evolution of the production rate of CO shows that it is dominated by the reversible reaction that regulates the interconversion between CO and CO_2, which is relatively slow. Even though more oxygen is available in leaner mixtures, the increase in mass flow rate leads to reduced residence times within the reaction front and consequently to an increase in the emitted CO.

Comparison of the results in Fig. 5 indicates that the predicted CO emissions are slightly higher for the case of the burner operating with the insulating cover, which is attributed to the favouring of the CO production by means of the CO_2 dissociation reaction in higher temperature environments.

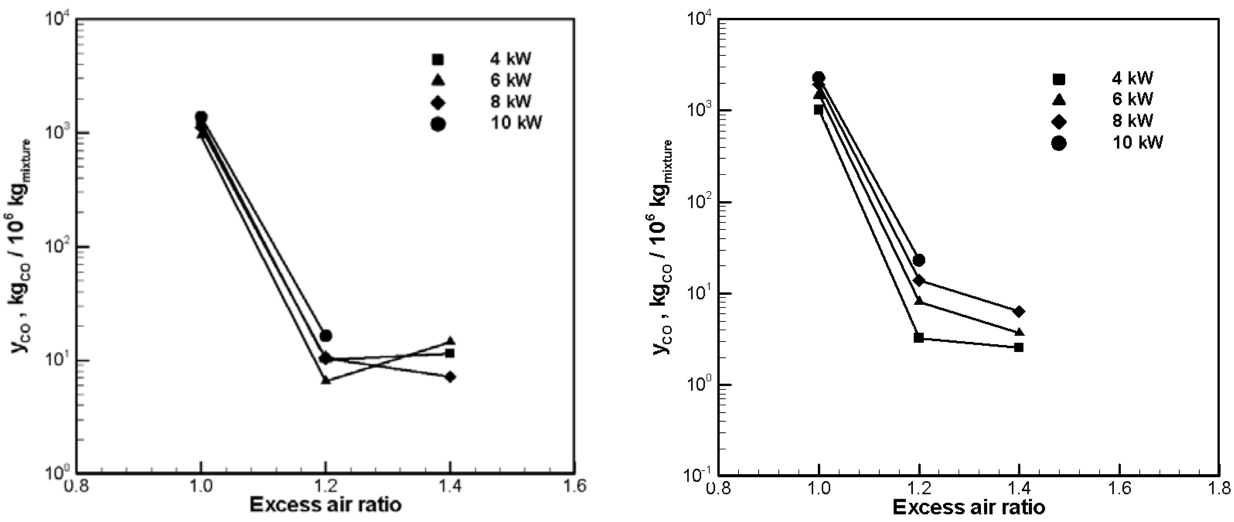

Figure 5. Predicted CO emission from burner, as function of the operating conditions. On the left, results for the burner operating uncovered. On the right, results are for burner facing a high temperature wall.

4. CONCLUSIONS

The three-dimensional numerical study of a two-layer porous burner is presented. The study aimed at investigating the influence of the outlet boundary condition on the performance of the burner. The three-dimensional Navier-Stokes equations were solved along with the equations of continuity, energy balances for both the solid and the fluid phases and transport of chemical species for a representative element corresponding to a 1/2463 fraction of the total volume of the combustion chamber. The model, which accounted for radiative heat transfer in the solid, convective heat exchange between the solid and the fluid phases, detailed chemistry of the oxidation of methane and detailed calculation of thermodynamic and transport properties, was solved by means of CFD techniques for a large set of operating conditions. Simulations were carried out for a set of operating conditions with power ranging from 4 to 10 kW and excess air ratio in the range from 1.0 to 1.4 and considering the burner radiating either to the environment or facing a hot wall placed downstream of it. The main results show that:

- For all the operating conditions considered, the peak temperature predicted for the burner operation facing a hot wall downstream of the outlet is higher than in the case of the burner open to the environment.
- The flame front remains within the flame support layer for both modes of operation. However, stabilization occurs closer to the interface between the two layers when the burner faces a hot wall.
- The predicted levels of NO emitted from the burner are higher for the burner facing a high temperature wall for all the operating conditions tested. Even though, NOx emissions are likely to attend stringent limits established for small gas fired water heating appliances, which confirms the advantage of using combustion in porous media.
- Predicted CO formation for the burner operation open to the environment indicates the existence of optimum operating conditions for which CO emission from the burner can be minimized. Predicted CO formation for the

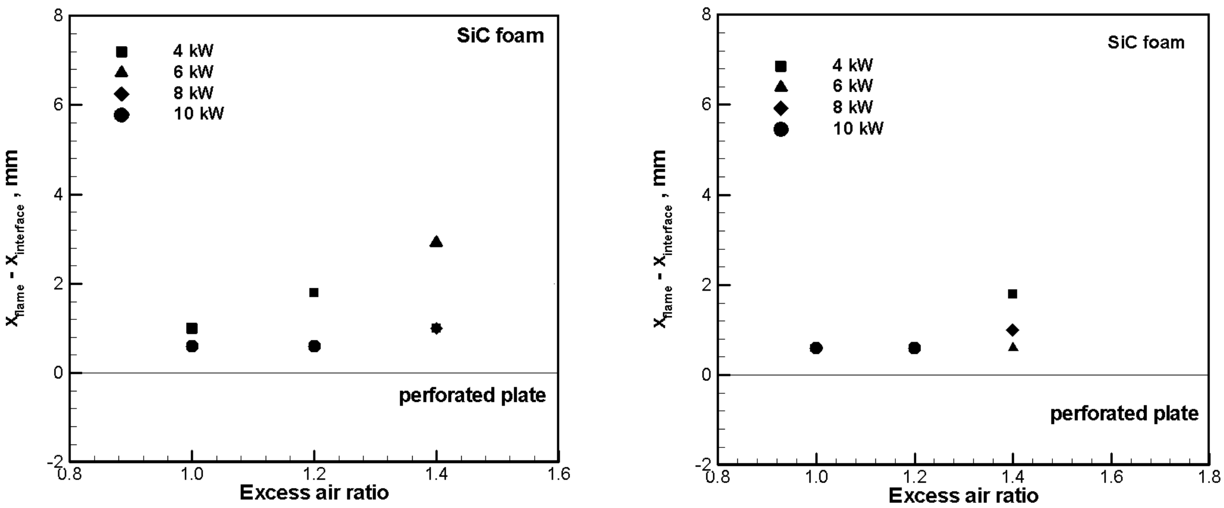

Figure 3. Flame position as function of the operating conditions. On the left, results are for the burner radiating to the environment. On the right are the results for burner facing a high temperature wall.

A comparison of the predicted emission of NO from the burner is presented in Fig. 4. It is shown that, regardless the heat transfer condition at the outlet boundary, NO emission increases with the thermal load for a constant excess air ratio. This was expected, since the main pathway for the production of this pollutant is the thermal-NO mechanism and thus, higher emission levels accompany the rise in temperature. Since NO is the main of the NOx pollutants formed in the burner, it is likely that NOx emission from the burner follow the same pattern. With the increase of the excess air ratio, more nitrogen is available in the reactants mixture. Even though, since temperatures decrease with the increase of dilution, the production of NO is reduced.

Regulations for the emissions of nitrogen oxides from house heating appliances vary widely among countries. Just for a comparison, Joynt and Wu (2000) report that NOx emission standard for natural gas fired water heaters are limited to 60 ng/J(input) in Austria, 34 ng/J in Japan and 26 ng/J in the case of residential appliances operated in California, USA. In the worst predicted case, corresponding to the operation of the burner covered at 10 kW-load and stoichiometric condition, the NO emission is 30 ng/J and thus below the less restrictive limits.

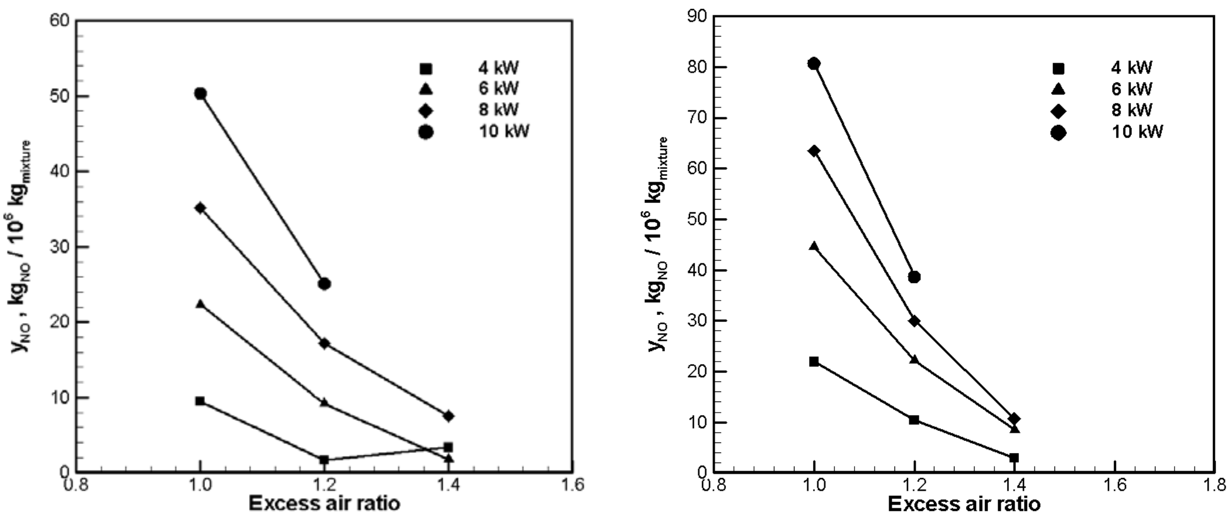

Figure 4. Predicted NO emission from burner, as function of the operating conditions. On the left, results for the burner operating open to the environment. On the right, results correspond to burner facing a high temperature wall.

In the same fashion, the predicted emission of CO from the burner is presented in Fig. 5 as function of the operating mode and outlet condition. It is observed that, for the two considered outlet condition, the increase of power is

3. RESULTS

Simulation of the burner was performed for a broad range of operating conditions considering either the burner operating open, radiating to a cold environment, or facing a hot wall. Calculation were accepted to be converged when normalized residues of all variables were lower than 0.01. This value was chosen as a compromise between accuracy and calculation time. Processing times, for typical runs (in a i686 Intel® Pentium® 4 processor type with 2.4 GHz) and 37268 grid points, ranged from 40 to 89 hours. The simulations of lower power and excess air ratio conditions were more time consuming.

In the calculations of the burner operating covered (i.e., facing a hot wall), the temperature of the wall placed downstream of the outlet of the SiC foam layer was imposed and made equal to measured value. It was observed that, accompanying the overall temperature, at the inner side of the cover, the temperature increases with power for a fixed excess air ratio and decreases with the increase in this coefficient when power is kept constant (Hayashi, 2005).

The influence of the operating conditions on the flame temperature, defined as the peak temperature, is presented in Fig. 2, for the two modes of operation studied. It is observed that higher flame temperatures are attained when the burner operates facing a hot wall. This was expected, since less heat is exchanged by radiation between the SiC foam and the environment in the latter case.

Figure 2 also shows that the flame temperature increases with power for a given excess air ratio. On the other hand, if the dilution of the reactants mixture is increased and the power kept constant, the peak temperature decreases. This is in agreement with the expected behavior of the burner.

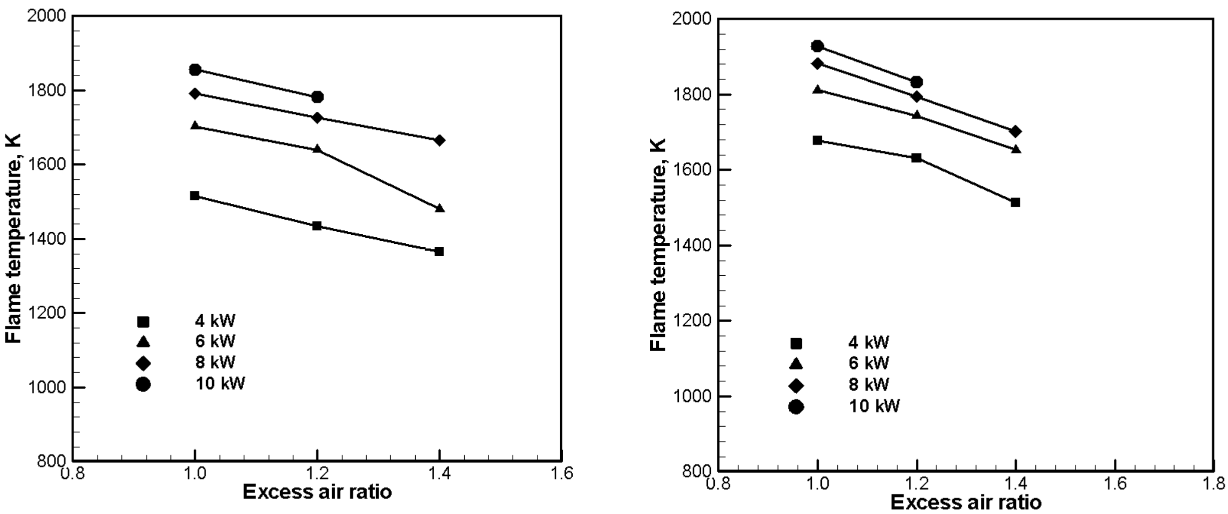

Figure 2. Flame temperature as function of the operating conditions. On the left, results for the burner operating uncovered. On the right, results are for burner facing a high temperature wall.

The flame position is defined as the point where the peak temperature is observed. It is presented in Fig. 3 as function of the operating mode and condition. Independently of the mode of operation, it is observed that the flame remains submerged within the SiC foam, close to the interface with the perforated plate, for the whole set of operating conditions tested. It is however noticed that the flame front tends to stabilize even closer to the interface between the two ceramic layers when the burner is operated with the cover. This is due to the increase in overall temperature observed in this case, which yields higher reaction rates and faster consumption of reactants and leads to the flame front moving upstream as a consequence.

y_k, M_k and h_k indicate, respectively, the mass fraction, molecular weight and specific enthalpy of the k-th species in the gas mixture, while $\mathcal{D}_{km}$ is the molecular diffusivity of species k in the mixture. Besides these, **v** is the phase averaged velocity vector, T_f and T_s are the fluid and solid temperatures, respectively, $(\nabla p)_p$ stays for the pressure loss owing to the presence of the porous matrix, h_v is the volumetric heat transfer coefficient, $(\nabla.\mathbf{q}_r)_p$ is the net thermal radiation flux within the porous material, and $\dot{\omega}_k$ is the rate of production of the k-th species in the course of the chemical reactions.

Closure models are required to estimate the unknown quantities in the governing equations. The pressure loss owing to the presence of the porous matrix was not considered in the perforated plate since, in this layer, direct calculation of the flow pathways is performed. In the SiC foam layer, this term was calculated by means of the Ergun equation as modified by Macdonald *et al.* (1979) and shown in Eq.(6) below, where d_p is the diameter of the pores.

$$(\nabla p)_p = 180\frac{(1-\varepsilon)^2}{\varepsilon^3}\frac{\mu\mathbf{v}}{d_p^2} + 1,8\frac{1-\varepsilon}{\varepsilon^3}\frac{\rho|\mathbf{v}|\mathbf{v}}{d_p} \qquad (6)$$

The radiative fluxes were calculated and imposed on the opaque walls of the perforated plate. The emissivity of these walls was taken from Modest (1993) and the gas that fills the holes was considered non-participating. The net radiative flux within the SiC foam was obtained by solving the radiative transfer equation, Eq. (7), for a homogeneous, emitting, absorbing and scattering medium. This was accomplished by application of the discrete ordinates method (see, *e.g.*, Modest, 1993). In Eq. (7), I_η is the radiant intensity at the wavelength η, $\hat{\mathbf{s}}$ is the unit vector in a given direction, κ_η stays for the absorption coefficient and β_η is the spectral extinction coefficient. Moreover, $\sigma_{s\eta}$ represents the spectral scattering coefficient, Φ_η is the spectral phase function and Ω_i is the solid angle, while the subscript b is used to refer to blackbody conditions. The medium was assumed to be grey and isotropically scattering, with properties taken from Mital *et al.* (1996).

$$\frac{dI_\eta}{ds} = \hat{\mathbf{s}}\cdot\nabla I_\eta = \kappa_\eta I_{b\eta} - \beta_\eta I_\eta + \frac{\sigma_{s\eta}}{4\pi}\int_{4\pi} I_\eta(\hat{\mathbf{s}})\Phi_\eta(\hat{\mathbf{s}}_i,\hat{\mathbf{s}})\,d\Omega_i \qquad (7)$$

The convective heat transfer coefficient for flow within the SiC foam was taken from Tong and Sathe (1991). For the perforated plate, a value of the superficial heat transfer coefficient for the flow inside the holes has been estimated, which was based on developing flow inside a duct at an average velocity in the range of operating conditions considered (Őzişic, 1985). Combustion was described by means of a skeletal mechanism for the oxidation of methane due to Glarborg *et al*. (1992), which is composed by 77 reactions involving 26 chemical species and accounts for the formation of nitrogen compounds.

Additionally, thermo-physical and transport properties of the reacting mixture were calculated with proper accounting for their dependence on temperature, pressure and composition by means of the use of the Chemkin code package for analysis of gas-phase chemical kinetics (Kee *et al*., 1995a) along with the Tranfit code package for evaluation of gas-phase multi-component transport properties (Kee *et al*., 1995b).

To complete the physical-mathematical model, proper boundary conditions had to be applied. In this work, the fluid velocity, temperature and composition were prescribed at the inlet section of the combustion chamber, and zero-gradient condition was assumed for all quantities in the far-field outlet boundary. Moreover, the temperature of the inlet and outlet planes of the solid layers were calculated with accounting for the radiation heat transfer with imaginary solid walls placed upstream and downstream of the calculation domain to include the interaction of the combustion chamber with the other components of the heating system. Symmetry conditions were imposed accross the y- and z-oriented boundary planes parallel to the main flow direction. Flow velocity was zeroed at the walls of the holes of the perforated plate, which were also considered impervious to the flux of chemical species.

The numerical implementation of the model was performed by integration of the differential equations in the computational domain with application of the finite volume/finite differences method and the SIMPLE algorithm (Patankar, 1980). The hybrid central/upwind scheme was applied in the discretization of the convective terms, while diffusive terms were discretized using central differences. The radiation problem consisted in the iterative solution of a set of 24 algebraic equations for each grid node, which was performed after every set of five overall iterations. To cope with the increased stiffness of the system of equations, which results of the large variation of the time scales that characterize the phenomena taking place simultaneously in the process, segregated solutions were obtained for the velocity, solid temperature and pressure profiles, while the gas temperature and concentration profiles were solved with application of the fractional time step method (Yanenko, 1971).

2.2. Geometric model

In order to be able to predict the three-dimensional flow, heat transfer and combustion at a reasonable computational cost, a 1/2463 fraction of the volume of the combustion chamber was considered. The modelled volume corresponds to a unit representative portion of the chamber, as shown in Fig. 1. As a geometrical simplification, the holes in the perforated plate have been represented by square cross-section holes with the same cross-sectional area of the actual cylindrical holes.

This approach allows for the two plates to be treated distinctly, taking into account in an adequate manner the very different porosities of the two media. While the SiC foam is modelled as a single continuum with volume-averaged properties, direct simulation of the fluid paths is applied to calculate the flow in the perforated plate.

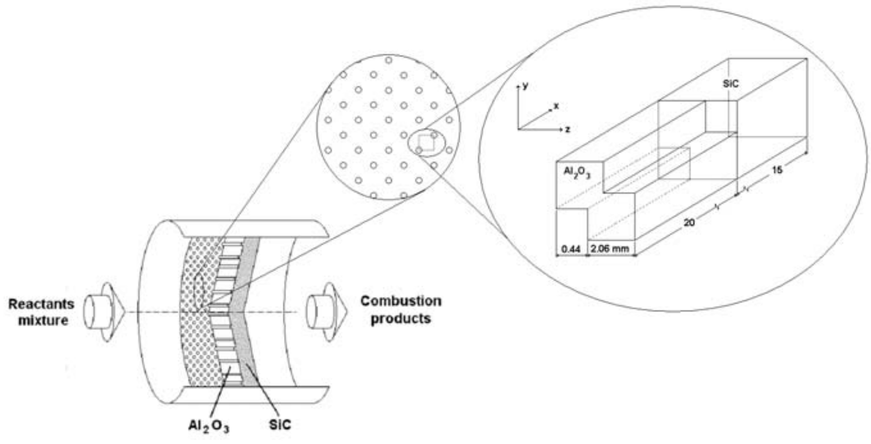

Figure 1. Schematic drawing of the two layer porous burner and representative unit cell.

2.3. Numerical model

The set of governing equations comprises the balances of overall mass of the mixture, momentum, energy and mass of each of chemical species for three-dimensional, steady, incompressible, laminar flow of a Newtonian fluid within an inert porous medium. Energy balances were performed for both the gas and the solid phases, since local thermal non-equilibrium is assumed. Catalytic effects of the high temperature solids were neglected. Radiative heat transfer was assumed to take place in the solid matrices but the gas was considered non-radiant. Thus, the volume averaged macroscopic forms of the continuity equation and of the balances of momentum, energy for gas and solid phases and transport of chemical species read, respectively, as:

$$\nabla\cdot\left(\varepsilon\rho_{\mathrm{f}}\mathbf{v}\right)=0 \tag{1}$$

$$\varepsilon\rho_{\mathrm{f}}\,\mathbf{v}\cdot\nabla\,\mathbf{v}=-\varepsilon\nabla p+\varepsilon\mu_{\mathrm{f}}\nabla\cdot\left(\nabla\,\mathbf{v}\right)-\left(\nabla p\right)_{\mathrm{p}} \tag{2}$$

$$\varepsilon\rho_{\mathrm{f}}\,c_{\mathrm{p,f}}\,\mathbf{v}\cdot\nabla\,T_{\mathrm{f}}=\varepsilon\nabla\cdot\left(k_{\mathrm{f}}\cdot\nabla\,T_{\mathrm{f}}\right)+h_{\mathrm{v}}\left(T_{\mathrm{s}}-T_{\mathrm{f}}\right)-\varepsilon\sum_{\mathrm{k=1}}^{N_{\mathrm{sp}}}\dot{\omega}_{\mathrm{k}}M_{\mathrm{k}}h_{\mathrm{k}} \tag{3}$$

$$0=\left(1-\varepsilon\right)\nabla\cdot\left(k_{\mathrm{s}}\nabla\,T_{\mathrm{s}}\right)-h_{\mathrm{v}}\left(T_{\mathrm{s}}-T_{\mathrm{f}}\right)-\left(\nabla\cdot\mathbf{q}_{\mathrm{r}}\right)_{\mathrm{p}} \tag{4}$$

$$\varepsilon\,\rho_{\mathrm{f}}\,\mathbf{v}\cdot\nabla\,y_{\mathrm{k}}=\varepsilon\,\rho_{\mathrm{f}}\nabla\cdot\left(\mathcal{D}_{\mathrm{km}}\cdot\nabla\,y_{\mathrm{k}}\right)+\varepsilon\dot{\omega}_{\mathrm{k}}M_{\mathrm{k}}\qquad \mathrm{k}=1,\ldots,N_{\mathrm{sp}}-1 \tag{5}$$

In Eq. (1) to Eq. (5), ρ_{f}, μ_{f}, $c_{\mathrm{p,f}}$ and k_{f} are the density, dynamic viscosity, specific heat capacity and the thermal conductivity of the fluid phase, respectively, while ε, ρ_{s}, $c_{\mathrm{p,s}}$ and k_{s} correspond to the void fraction (or porosity), the density, the specific heat capacity and the thermal conductivity of the solid phase, respectively. In addition, flame burner (Viskanta and Gore, 2000). Numerical simulations on the performance of this innovative burner have already been reported, having available experimental data been used to validate the developed computational models (Hayashi, 2005, Hayashi *et al.*, 2004, 2007). Through the study of several operating conditions and porous media characteristics, numerical simulation is shown to play an important role in the development of porous burners, providing guidance for the improvement of existing configurations and for the proposition of new designs.

Downstream conditions are among the several parameters that affect the performance of porous burners. Lammers and de Goey (2003) studied this influence for a ceramic-porous surface burner (i.e., a burner where the flame is stabilized near the outflow interface of the porous media). Their analysis is based on a one-dimensional model that accounts for complex chemistry and radiation inside the ceramic foam. It was shown that when the porous burner was operated in a very hot environment flashback of the flame could occur and the flame could enter the porous media, which was not desired in that case.

The numerical results reported in Hayashi *et al.* (2004, 2007) considered that the porous burner radiates to a cold environment. This outlet condition characterizes the situation where the porous burner acts as a radiant burner. Despite radiant heating being the most common application for porous burners, the objective of the burner presented in this study is the heat transfer between the hot combustion products and a process fluid circulating through a heat exchanger. The burner is part of an innovative heating system, which also incorporates a cool flame vaporizer upstream and a multi-jet boiler downstream of the combustion chamber. When the porous burner is part of this assembly, it operates facing a high temperature wall, which affects the radiative heat losses of the burner. In order to assess the influence of the high temperature wall downstream of the burner, two different conditions were studied: *i)* the burner operating uncovered and radiating to a cold environment and *ii)* the burner operating covered by an insulated surface as to resemble the existence of a hot facing wall.

2. MODEL

2.1. Problem formulation

The porous burner under study was designed and built at the Laboratory of Fluid Mechanics – LSTM, of the University of Erlangen-Nürnberg, in Germany, as part of the development of an innovative system for household heating. The new heating device incorporates the technologies of cool-flame vaporization and combustion within porous media, along with a high efficiency multi-jet heat exchanger and control systems (Brehmer *et al.*, 2003), resulting in a compact, high efficiency equipment suitable to operate at a large turndown ratio. The cool flame vaporizer converts a fine spray of liquid fuel to a mixture of gaseous fuel and air, which is fed to the combustion chamber, the porous burner. Downstream of the burner, the hot combustion products are admitted in the heat exchanger in order to heat a water jacket. The gas-side of the boiler consists of a series of inserts supplied with holes in their lateral walls, which are parallel to the axial direction, while the bottom walls of the inserts are positioned perpendicularly to this streamwise direction. This inserts are kept aligned and are fixed such that the gas stream is deflected at the bottom wall of the elements, being directed to the lateral perforated walls, in a way to promote the impingement of jets on the target boiler walls. The jets are deflected in the annular region between the lateral wall of each insert and the wall of the boiler, being thus directed to the subsequent insert. It is the existence of this boiler downstream of the porous burner that motivates the present study. When the porous burner is assembled in the heating system, it faces a high temperature wall, the bottom wall of the first insert. This fact has implications on the performance of the porous burner and to study them a numerical investigation was performed. The studied porous burner consists of a 15 mm-thick slab of silicon carbide foam presenting 90% void fraction, preceded by a perforated plate made of alumina with 20 mm in thickness. The perforated plate serves to homogeneously feed the premixed air-fuel reactive mixture to the SiC foam, the flame support layer. It is made of an insulating material to also prevent flashback of the flame front towards the burner inlet. The holes are 1 mm in diameter and are uniformly distributed, yielding a 4% equivalent porosity.

Porous media are often treated as a single continuum with volume-averaged properties (Kaviany, 1995), which allows for one- or two-dimensional simulations of the porous burner. This was the approach followed for the silicon carbide foam. However, the perforated plate could not be replaced by a homogeneous porous media with 4% porosity. Besides the error introduced in assuming the perforated plate to be a homogeneous medium, which is a strong simplification, the very low porosity of the medium leads to a significant decrease in the advective contribution in the energy balance of the gas phase, because the phase-averaged velocity is very low. Indeed, modelling of the perforated plate as a single continuum with very low porosity is inadequate, since the solution of the volume-averaged equations yields the phase averaged velocity field, i.e., the mean velocity in a clear pipe of the same cross sectional area of the porous element. This velocity is much lower than the mean velocity in the small diameter holes of the perforated plate, and yields solutions in which the flame front stabilizes in the first half (actually, it is anchored very close to the inlet section) of this layer, which is an unrealistic result (in the perforated plate, the Péclet number is lower than 65, which is the value above which combustion inside the pores is possible (Babkin *et al.*, 1991)).

As a consequence of the above explanations, the interest to investigate the detailed flow at the interface of the two plates brought about the need to model the flow within the holes by means of a three-dimensional model.

INFLUENCE OF THE DOWNSTREAM CONDITIONS ON THE PERFORMANCE OF A TWO-LAYER POROUS BURNER

Thamy Cristina Hayashi, thamy@ufba.br
Federal University of Bahia, Dept. of Chemical Engineering, R. Aristides Novis, 2, Federação, 40210-630, Salvador, BA, Brazil

Isabel Malico, imbm@uevora.pt
University of Évora, Dept. of Physics, R. Romão Ramalho, 59, 7000-671, Évora, Portugal

José Carlos Fernandes Pereira, jcfpereira@ist.utl.pt
Instituto Superior Técnico, Dept. of Mechanical Engineering, Av. Rovisco Pais, 1049-001, Lisbon, Portugal

Abstract *Bilayered porous burners are characterized by being constituted of two porous layers of different porosity. The flame front is stabilized within the higher porosity layer, which is preceded by another layer with pores of smaller diameter. An innovative two-layer porous burner that integrates a newly designed household heating system is numerically studied. The bilayered porous burner studied in this work integrates an innovative household heating system, also composed of a cool flame vaporizer and a multi-jet boiler. As a consequence of this assembly, it operates facing a high temperature wall, which affects the radiative heat losses of the burner. In order to assess the influence of this high temperature wall downstream of the burner outlet section on the performance of the burner, a numerical study of the flow and heat transfer within the combustion chamber was conducted by means of a three-dimensional model of a unit cell representative of the geometry of the two-layered porous burner. The model includes the Navier-Stokes equations, the gas and solid energy balances and the transport equations for chemical species and was computationally implemented using the finite volume/finite differences method. Radiation heat transfer in the solid matrices and local thermal non-equilibrium are accounted for. Additionally, detailed reaction mechanisms are applied to model the combustion process, allowing for the prediction of the pollutants formation. Calculations of the burner over a broad range of operating conditions were conducted, considering either the existence or not of a high temperature wall downstream of the burner outlet. A comparison of the performance of the burner showed that operation facing the high temperature wall: i) promotes the stabilization of the flame front deeper inside the higher porosity ceramic foam, close to the interface of the porous layers for all the range of operating conditions and ii) results in higher peak temperatures and NO and CO emissions.*

Keywords*: Porous burner, Combustion in porous media, CFD*

1. INTRODUCTION

Combustion has been mankind's major source of heat for either end-use as so or conversion to work. Even though research on alternative energy sources have been reinforced in the past decades, the availability of fossil fuels has made it very difficult for other technologies to prove being more reliable and cost-effective than simply burning coal, oils and natural gas or other hydrocarbon fuels. Nevertheless, it has become well known that fossil fuel reserves are limited and efficient use of the energy resources is imperative. Moreover, regulations on limits for greenhouse gases emitted from combustion processes are becoming more and more stringent worldwide. This scenario has provided the motivation for most research effort on new combustion technologies or for the improvement of existing ones. Within this context, combustion in porous media has emerged as an efficient way to convert the chemical energy of combustible into sensible heat of gases or enhanced radiation heat flows (Howell *et al.*, 1996 and Viskanta and Gore, 2000).

Combustion in porous media is based on the recuperation of heat from the region beyond the flame zone to preheat the reactants mixture upstream of the flame position. It thus involves intimate interaction of the local heat release owing to the chemical reactions with the three modes of heat transfer. This internal feedback of heat from the combustion products to the premixed reactants stream results in higher burning speeds and in the extension of the lean flammability limit, in comparison to conventional unconfined flames. This ability to operate at higher excess air ratios, i.e. with more diluted mixture conditions, contributes to the lowering of emission of pollutants, namely CO and NOx, which is characteristic of this combustion technique. Moreover, compared to open flame burners, porous combustors present higher efficiencies and broad turndown ratio, allied with compactness. These characteristics of combustion in porous media also bring about the possibility of burning fuels of lower heating values, as well as unconventional fuels like, for instance, those obtained from residues. Several experimental and numerical studies have demonstrated the practical benefits of porous burners (e.g., Kotani *et al.*, 1984; Hsu *et al.*, 1993; Mößbauer *et al.*, 1999; Durst and Trimis, 2002; Al-Hamamre *et al.*, 2006).

In this work, a study focused in a new design of a porous combustor is presented. Considering its configuration, the combustor is characterized as a two-layer porous burner, since it is made up with two plates made of porous materials with different properties. Because the flame is to be anchored deep inside the porous slab made of a high porosity ceramic foam, close to the interface between the plates, the combustor is also classified as a submerged (or embedded)